

Fabrication of silicon microwires by a combination of chemical etching steps and their analysis as anode material in Li-ion batteries

Oscar Pérez-Díaz, Enrique Quiroga-González, Sandra Hansen, Nicolás Rutilo Silva-González, Jürgen Carstensen & Rainer Adelung

To cite this article: Oscar Pérez-Díaz, Enrique Quiroga-González, Sandra Hansen, Nicolás Rutilo Silva-González, Jürgen Carstensen & Rainer Adelung (2019) Fabrication of silicon microwires by a combination of chemical etching steps and their analysis as anode material in Li-ion batteries, *Materials Technology*, 34:13, 785-791, DOI: [10.1080/10667857.2019.1629059](https://doi.org/10.1080/10667857.2019.1629059)

To link to this article: <https://doi.org/10.1080/10667857.2019.1629059>



Published online: 11 Jun 2019.



Submit your article to this journal [↗](#)



Article views: 57



View related articles [↗](#)



View Crossmark data [↗](#)



Fabrication of silicon microwires by a combination of chemical etching steps and their analysis as anode material in Li-ion batteries

Oscar Pérez-Díaz^a, Enrique Quiroga-González^a, Sandra Hansen^b, Nicolás Rutilo Silva-González^a, Jürgen Carstensen^b and Rainer Adelung^b

^aInstitute of Physics, Benemérita Universidad Autónoma de Puebla, Puebla, México; ^bInstitute for Materials Science, Functional Nanomaterials, Kiel University, Kiel, Germany

ABSTRACT

This work presents a thorough study of Si microwires obtained by a novel combination of chemical etching steps, for their application as anode material in Li-ion batteries. The fabrication process starts with standard photolithography followed by a metal-assisted chemical etching step and anisotropic etching. This process can be performed in any chemical laboratory. The final structures possess a diameter and a length of 1.5 and 24 μm , respectively. Paste electrodes were prepared using the Si microwires and were tested in half-battery cells. Cyclic voltammetry and impedance spectroscopy evidenced the formation of Li–Si alloys and a solid electrolyte interface. The lithiated wires are mechanically stable upon lithiation, even when they expand to the 256% of their original volume.

ARTICLE HISTORY

Received 1 February 2019
Accepted 2 June 2019

KEYWORDS

Li ion battery; Si microwires; metal assisted chemical etching; impedance spectroscopy; mechanical stability

Introduction

Recently, the most commonly used anode material in Li batteries is graphite due to its low production cost, but it can only provide a capacity of 370 mAh/g [1] because it can only store one Li atom per each six of C. In recent years, a series of materials have been studied for replacing graphite [2,3]. These materials consist of metallic alloys between Li and M ($M = \text{Sb, Pb, Si, Ge, Sn, In}$) that in principle offer more gravimetric capacity than graphite [4,5]. Si offers a capacity of 4200 mAh/g [6,7], the highest for anode materials. Although Si capacity is more than 10 times that of any existing graphite-based anode, it is useless as an anode in its bulk state, since it pulverises after some charge/discharge cycles due the volume expansion (up to 300%).

The solution to this problem is to micro- or nano-structure it to withstand the volume change. Some of the possible structures are nanowires [4], nanopillars [8], microwires [6] or thin films [7] to name a few. Among these structures, the most promising form in which Si can be used as an anode for Li-ion batteries is in microwires. This kind of structure allocates the volume changes in two dimensions, with higher capacities given by the volume and lower surface effects than in nanowires. Quiroga-González et al. obtained an array of Si microwires by a sequence of steps that consist of lithography and pre-structuring of Si wafers, electrochemical etching of macropores followed by a chemical over-etching, deposition of a Cu current collector and the detaching of the anode from the Si substrate [6]. These Si microwires

proved to allow the volume expansion, exhibiting a stable capacity of 3150 mAh/g for 100 cycles of charging/discharging [9]. Additionally, the Si microwire arrays of this kind, with a length of only 70 μm , possess an areal capacity (the amount of charge that the electrode can store per nominal area) larger than any other form of Si anodes, at very high charge density rates (charge stored per unit of area of the electrode per unit of time). For example, Si nanowires have presented an areal capacity of 0.52 mAh/cm² at a charge density rate of 0.17 mAh/cm²h [10], while the value for Si microwires is of 5.67 mAh/cm² at 2.84 mAh/cm²h [11].

The microstructures mentioned above are a good option to be applied as an anode in Li-ion batteries; nevertheless, their fabrication method requires equipment that could not be found in every laboratory. In the present work, Si microwires were fabricated by an alternative method that consist of a combination of two methods: metal-assisted chemical etching of Si in HF-based solutions to form micro and nanowires, and anisotropic over-etching of the nanowires in KOH-based solutions. Paste electrodes were fabricated and tested in half-cells batteries. Cyclic voltammetry was used to find the potential window to operate the anodes while impedance spectroscopy helped in the identification of the interfaces of the anode assembled in a battery, and how they change when the anode is totally lithiated. Ex situ SEM analyses were performed after Si is fully lithiated, to elucidate the mechanical stability of the microstructures.

Production process of Si microwires

The process to obtain the Si microwires consists of the sequence of steps listed below (see Figure 1):

- (1) Pre-structuring a Si wafer by conventional UV lithography (Figure 1(a)).
- (2) Chemical deposition of noble metal particles (Figure 1(b)).
- (3) Etching process in an HF-H₂O₂ based solution (Figure 1(c)).
- (4) Over-etching in a KOH-based solution (Figure 1(d)).

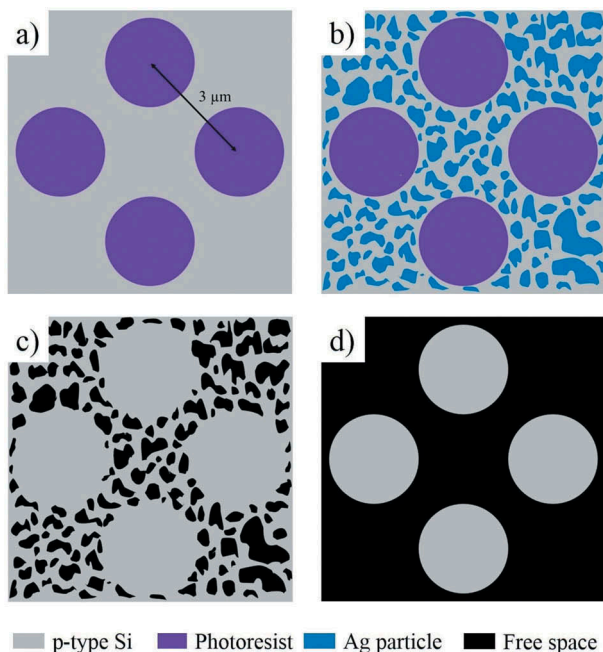
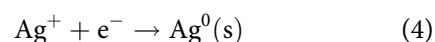
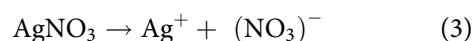
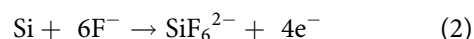


Figure 1. Schematic of the methodology for the fabrication of arrays of Si microwires.

First, a quadratic array of circles of photoresist is transferred to a Si wafer, with a distance between the centres of the circles of 3 μm. It is important to mention that p-type Si (100) wafers with a resistivity of 15–25 Ω cm are used as starting material. The circles of photoresist act as a masking layer for the metal deposition and the subsequent etching process. On step 2, the pre-structured wafer is immersed in an AgNO₃ 0.01 M aqueous solution containing 2 mL of HF 48% v/v for every 100 mL of solution. Ag deposits on the sections without photoresist (Figure 2(a)). The cubes of the figure correspond to the photoresist, whereas the parts between them correspond to the Si surface now covered with Ag particles. The Ag⁺ ions are reduced and form metallic Ag particles on those areas where there is no photoresist. The reactions occurring during the deposition process are indicated below [12–14]:



It can be seen that the entire surface is covered by particles with sizes ranging from 14 to 300 nm (see the inset in Figure 2(a)). The presence of particles with sizes below 50 nm could produce (with highest probability) that the etching process occurs at

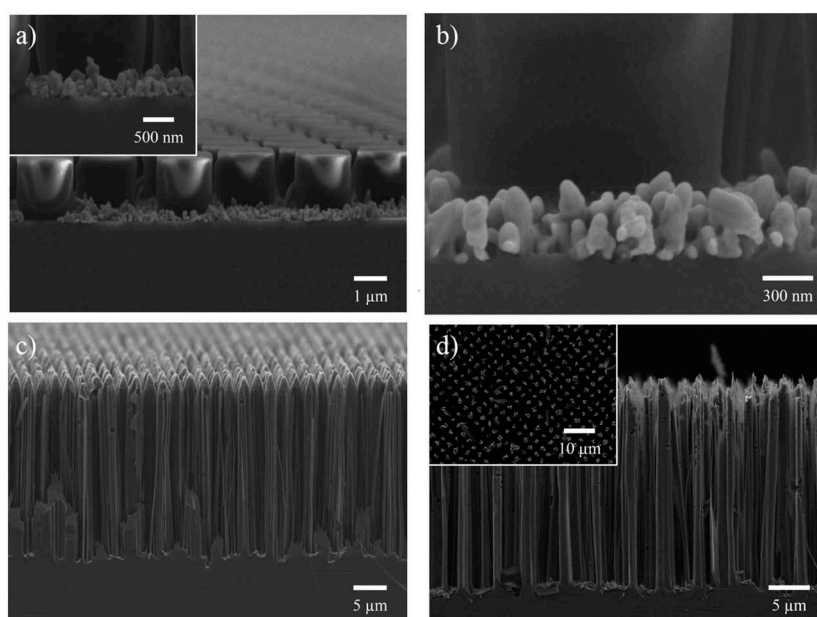
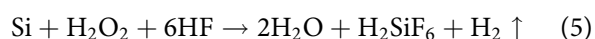


Figure 2. SEM micrographs obtained after every step for fabricating the Si microwires: (a) Ag particles deposited on Si surface, (b) pre-etching step and smaller Ag particles dissolution in HNO₃, (c) main etching process and (d) final Si microwires arrangement. Two columns.

directions different than the transversal one, generating lateral pores [15,16], that can be detrimental for the production of the structures. To avoid lateral etching, it is necessary to remove the smallest particles. To do this, the sample is first submitted to a pre-etching step, to allow the bigger particles encrusting in Si. The pre-etching is performed by immersing the sample into an etching solution of HF 48%, H₂O₂ 30% and deionised water in a proportion of 8:1:71 v/v at 30°C for 30 s. Afterwards, the smaller Ag particles are dissolved by immersing the sample in a solution of HNO₃ and deionised water in a proportion 1:3 v/v for 30 s [17]. The etchant attacks all the Ag particles, but the smaller particles are dissolved much faster because of their higher surface to bulk ratio. Figure 2(b) exhibits the sample after the pre-etching step and the dissolution of the smaller Ag particles. The bigger particles are encrusted in the Si substrate at a depth of 360 nm.

After a cleaning process in deionised water, the sample is submitted to the main etching process. The etching solution is the same as the one used in the pre-etching step, but the time for this step is 1 h. The etching takes place where the Ag particles are. Due to the high oxidation potential of H₂O₂, the Si surface is oxidised underneath the metal particles, and this oxide is simultaneously dissolved by the HF. As Si is continuously oxidised and dissolved around the particles, the wafer is etched to form Si nanowires in the interstices between Ag particles, and micro-wires in the zones (defined by lithography) free of Ag. In Figure 2(c), the sample after the etching process is shown. The sections where Si was etched present Ag particles at the bottom. The reaction that rules etching process is [18]:



In order to obtain a sample with only Si microwires, it is necessary to remove the sections with nanowires. This is accomplished in a 0.25 wt% (weight percent) aqueous solution of KOH at 50°C for 1.5 h. The etching takes place in the entire sample, but as the nanowires are much thinner, they are dissolved faster than the microwires. In Figure 2(d) the final array of Si microwires is presented. The inset of this figure is a micrograph of the surface of the array. The final structures present a length of 24 µm and a diameter of 1.5 µm. Certain porosity can be observed at the top of the structures, suggesting that lateral etching was not completely avoided. Nevertheless, structural integrity is conserved.

Preparation of paste anodes and half battery cells

Paste electrodes were fabricated. For this purpose, Si microwires are scratched from the substrate and

mixed with carbon black (CB), carboxymethyl cellulose (CMC) and water. To study the processes occurring in the Si microwires, the limitation of the electronic transport to the Si microwires was minimised by using an excess of CB (compared to conventional amounts for preparation of electrodes). The proportion of CB:Si:CMC was 45:45:10 in weight, as in previous reports [19]. The CB provides electrical contact between the microwires and the CMC is the binder. A layer of the paste is casted on a Cu foil, and the produced sample is dried at 90°C for 12 h in a hot air oven. The Cu foil acts as the current collector. In Figure 3 an SEM micrograph of the paste is presented. As can be seen, Si microwires are completely surrounded by CB.

The fabricated anodes were tested in half cells using metallic Li as a counter electrode. The electrolyte was a solution 1 M of LiPF₆ in ethylene carbonate and dimethyl carbonate in a proportion 50:50 v/v. A Whatman filter paper was used as a separator.

Electrochemical characterisation

Cyclic voltammetry

Cyclic voltammetry tests were performed at a scan rate of 100 µV/s in a range of 10 mV to 1.5 V for three cycles. The resulting voltammogram is shown in Figure 4. Its shape is similar to those reported in previous studies where Si was used as anode [20–22]. The observed peaks correspond to the formation of Si–Li alloys and a solid electrolyte interface (SEI) [23]. The peak A (at around 0.6 V) corresponds to a non-reversible process, since only appears in the first cycle, in the negative voltage sweep. The process is related to the formation of SEI [9], composed of decomposition products of electrolyte and Si. The peaks below 0.60 V correspond to reversible processes associated with Si–Li alloys; in other words,

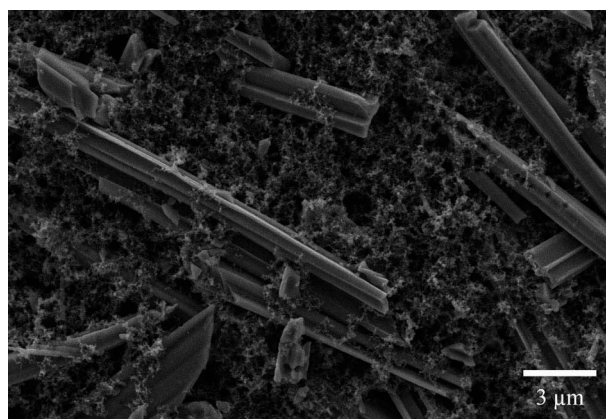


Figure 3. SEM micrograph of a paste electrode with Si microwires. It is possible to observe that Si microwires are completely surrounded by CB, warranting a good electric contact between them. One column.

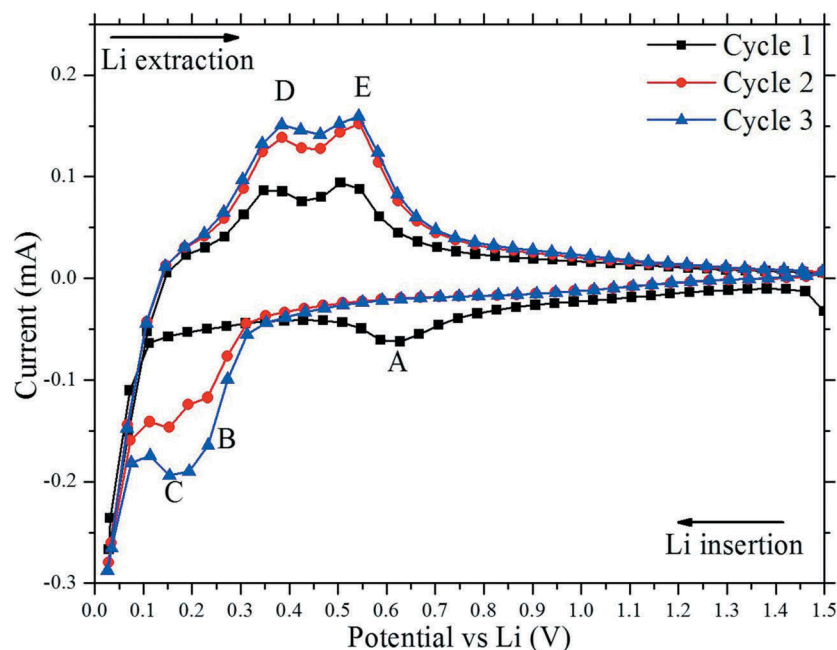


Figure 4. Cyclic voltammogram of Si microwires in paste anodes. A not reversible event takes place only in the first cycle at 0.61 V, related to the SEI formation. Additionally, the lithiation peaks B and C at 0.25 V and 0.16 V, and the delithiation peaks D and E at 0.38 V and 0.53 V are observed. One column.

Li is inserted into Si resulting in phase transformations and voltammetric peaks. At 0.25 V peak, B appears, which represents a partial lithiation of Si in the form of the $\text{Li}_{13}\text{Si}_4$ phase [15,24]. At 0.16 V (peak C), it is possible to find the $\text{Li}_{22}\text{Si}_5$ phase [24,25] (the fully lithiated Si phase).

The positive peaks correspond to the delithiation process. Peak D, 0.38 V, corresponds to the partial extraction of Li (Li_xSi_y phases), while the peak at 0.53 V (peak E) corresponds to the full extraction of Li from Si [24]. From these results, it is possible to determine that the potential window for operation of the electrode is from 0.1 to 0.7 V.

CMC and CB do not present any visible interaction with Li. Hansen *et al.* showed that even with big amounts of CB into the paste, no voltammetric peaks related to interactions of this material with Li are found [13].

Impedance spectroscopy

Impedance spectroscopy (IS) was performed in a frequency range of 2 Hz to 500 KHz using a small signal of 50 mV. In Figure 5(a) the Nyquist plot of a fresh-assembled battery is presented. An electrical model consisting of three RQ circuits (3-time

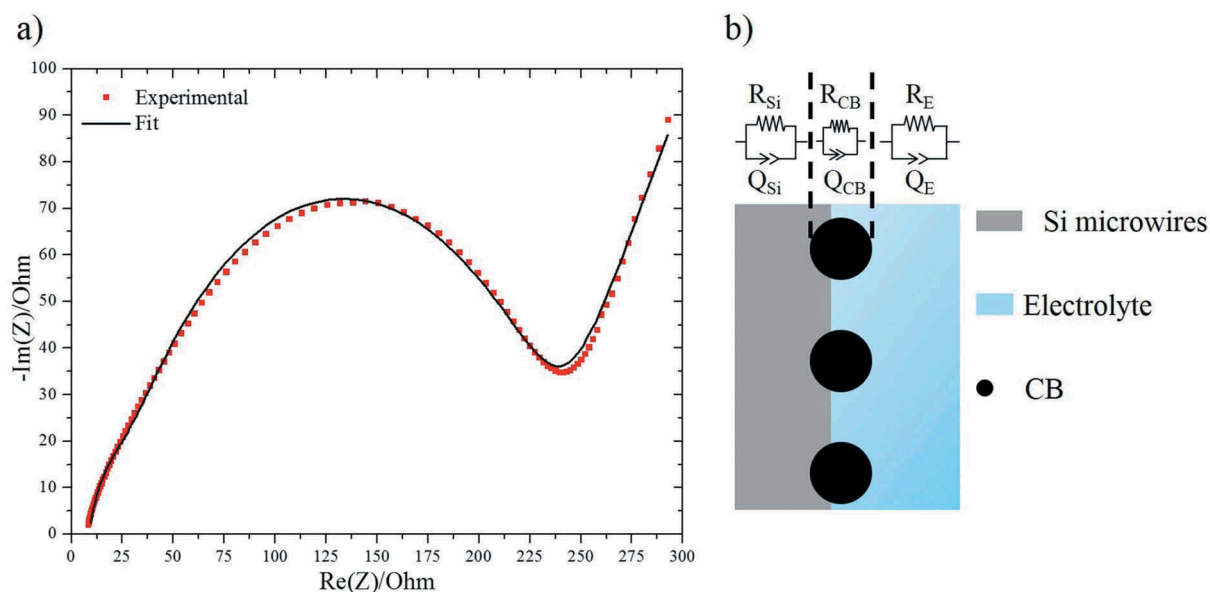


Figure 5. (a) Nyquist plot of a fresh-assembled battery. (b) Equivalent circuit representation of the battery. Two columns.

constants) in series plus a series resistance could be fitted to the IS data. Q is a constant phase element. In Figure 5(b) a schematic of the elements of the cell is presented. The series resistance can be attributed to the connections (cables, elements of the cell, etc.). After determining the time constants, it was possible to identify two fast processes (of 120.56 and 2.58 ms) and one slow (of 2.17 s). The slowest time constant can be related to the charge transfer to the Si microwires (τ_{Si}). The faster time constants may refer to electronic conduction through the conducting matrix (τ_M) composed of CB and the CMC [13], and to the ionic conduction through the electrolyte (τ_E).

IS was also performed on a battery after Si was fully lithiated. For this purpose, a current density of 161.5 mA/g (C/26) was applied to the battery until the voltage reached 0.1 V (the potential at which the phase with the highest Li content is obtained); then a constant potential of 0.1 V was applied for 12 h. Figure 6(a) presents the respective Nyquist plot. As it can be seen, the shape of the spectrum is different to the one of a fresh battery (with unlithiated Si). This happens because the elements of the battery change, with the exception of the electrolyte. The microwires are not composed of Si anymore, but of a Si-Li alloy, and an SEI is formed around the wires [26,27]. In this case, it was also possible to use the electric model used for the fresh-assembled battery [14]. Three-time constants were identified. The slowest one (18.58 ms) corresponds to the charge transfer to the Si-Li microwires. The other two can be associated with the electrolyte, that in principle does not suffer change (2.58 ms), and to the SEI layer containing CB (1.85 ms). The SEI layer is in parallel to the CB matrix; thus, it is not possible to distinguish between these two elements, but the higher value of Q produces a higher time constant than the one

attributed to the transport through CB. Figure 6(b) shows a schematic of the elements of the cell after the lithiation process.

Mechanical stability

Figure 7 shows an SEM micrograph of the Si microwires after full lithiation (using the same lithiation procedure as above). The wires changed their original diameter from 1.5 to 2.4 μm , representing a volume expansion to 256%. The diameter of 2.4 μm is similar to the diameters obtained when lithiating solid Si microwires with diameters of 1.5 μm [15].

To better elucidate the volume changes, the microwires were lithiated in an array (without CB nor CMC). In this case, the wires are still attached to the Si substrate. Figure 8 shows the microwires before and after the Li insertion. It is possible to observe that

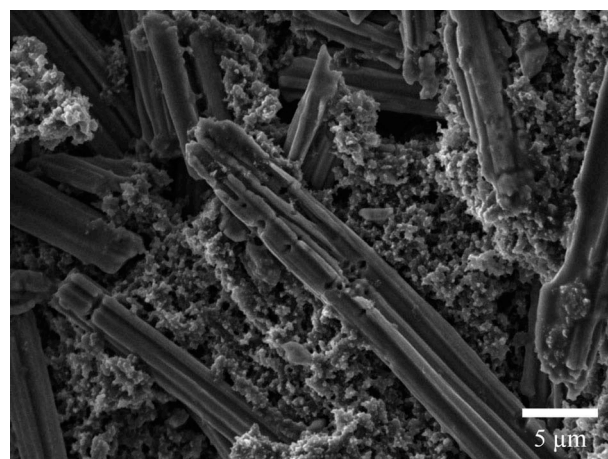


Figure 7. SEM micrograph of Si microwires in a paste electrode after Li insertion. One column.

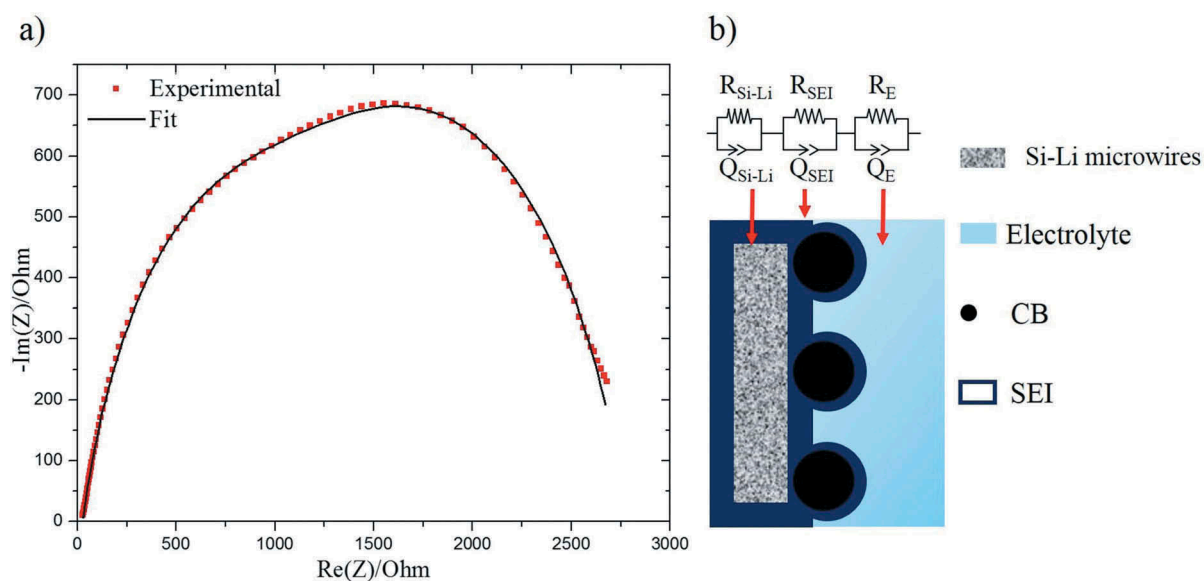


Figure 6. (a) Nyquist plot of a battery with fully lithiated Si microwires. (b) Equivalent circuit representation of the battery. Two columns.

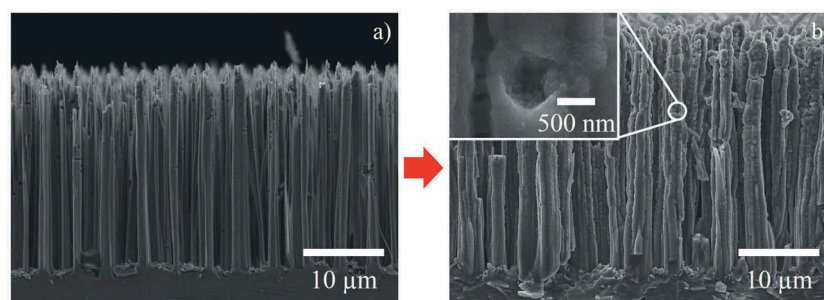


Figure 8. SEM micrographs of an array of Si microwires (a) before Li insertion and (b) after Li insertion. The inset shows a filled pore due to volume expansion given by the formation of Si–Li alloys. Two columns.

the shape of the structures is conserved. The top of the wires is thinner, probably due to the higher density of lateral pores in those sections. The pores may allocate the volume changes during lithiation.

Conclusions

A thorough study of Si microwires obtained only by chemical etching steps was presented, with the aim to use them as anode material in Li-ion batteries. The structures have a diameter of 1.5 µm and a length 24 µm. The top of the wires is porous, even when the probability of producing lateral pores was minimised by optimising the fabrication conditions. However, the structural integrity of the microwires is conserved. Paste anodes were fabricated using the microwires, CB and CMC, and then tested in half-cells. It was possible to determinate that the potential window for operation of the anodes is in the range of 0.1 to 0.7 V. SEI is formed just during the first cycle, as identified through a non-reversible voltammetric peak at 0.6 V. Impedance spectroscopy was performed in order to study the behaviour of the electrode when the battery was fresh assembled and when Si was fully lithiated. An electric circuit was used to model the impedance responses and in both cases consisted of three RQ circuits in series plus a series resistance. However, when the battery was fully lithiated, the elements of the cell were not the same: after lithiation the microwires were composed of a Li–Si alloy and SEI layer was on their surface. This produced a change in the time constants. The wires are mechanically stable even when submitted to a volume expansion to 256% during lithiation. Lithiated wires have an average diameter of 2.4 µm, being the top of them relatively thinner due to the porosity of this section (the porosity could allocate volume changes).

Acknowledgments

This work was funded by projects CONACyT INFR-2011-1-163153, CONACyT CB-2014-01-243407 and PROMEP BUAP-NPTC-377. O.P.-D. acknowledges the financial support of CONACyT through the scholarship number 378447.

Disclosure statement


No potential conflict of interest was reported by the authors.

Funding

This work was supported by the PROMEP [BUAP-NPTC-377];CONACyT [CB-2014-01-243407];CONACyT [INFR-2011-1-163153];CONACyT [378447].

ORCID

Oscar Pérez-Díaz  <http://orcid.org/0000-0001-5295-1412>
Enrique Quiroga-González  <http://orcid.org/0000-0003-1650-0862>

Nicolás Rutilo Silva-González  <http://orcid.org/0000-0001-8337-1461>

References

- [1] Scrosati B. Recent advances in lithium ion battery materials. *Electrochim Acta*. 2000;45:2461–2466.
- [2] An Y, Fei H, Zeng G, et al. Green, scalable, and controllable fabrication of nanoporous silicon from commercial alloy precursors for high-energy lithium-ion batteries. *ACS Nano*. 2018;12:4993–5002.
- [3] Tian Y, An Y, Feng J. Flexible and freestanding silicon/mxene composite papers for high-performance lithium-ion batteries. *ACS Appl Mater Interfaces*. 2019;11:10004–10011.
- [4] Peng KQ, Wang X, Li L, et al. Silicon nanowires for advanced energy conversion and storage. *Nano Today*. 2013;8:75–97.
- [5] Osiak M, Geaney M, Armstrong E, et al. Structuring materials for lithium-ion batteries: advancements in nanomaterial structure, composition, and defined assembly on cell performance. *J Mater Chem A*. 2014;2:9433–9460.
- [6] Quiroga-González E, Ossei-Wusu E, Carstensen J, et al. How to make optimized arrays of Si wires suitable as superior anode for li-ion batteries. *J Electrochem Soc*. 2011;158:E119–E123.
- [7] Chen LB, Xie JY, Yu HC, et al. An amorphous Si thin film anode with high capacity and long cycling life for lithium ion batteries. *J Appl Electrochem*. 2009;39:1157–1162.
- [8] Huang R, Fan X, Shen W, et al. Carbon-coated silicon nanowire array films for high-performance

- lithium-ion battery anodes. *Appl Phys Lett*. 2009;95:133119-1-133119-3-2.
- [9] Quiroga-González E, Carstensen J, Föll H. Good cycling performance of high-density arrays of Si microwires as anodes for Li ion batteries. *Electrochim Acta*. 2013;101:93-98.
 - [10] Ruffo R, Hong SS, Chan CK, et al. Impedance analysis of siliconnanowire lithium ion battery anodes. *J Phys Chem C*. 2009;113:11390-11398.
 - [11] Quiroga-González E, Carstensen J, Föll H. Optimal conditions for fast charging and long cycling stability of silicon microwire anodes for lithium ion batteries, and comparison with the performance of other si anode concepts. *Energies*. 2013;6:5145-5156.
 - [12] Kang K, Lee H, Han D, et al. Maximum Li storage in Si nanowires for the high capacity three dimensional Li-ion battery. *Appl Phys Lett*. 2010;96:0531101.
 - [13] Hansen S, Quiroga-González E, Carstensen J, et al. Size-dependent cyclic voltammetry study of silicon microwire anodes for lithium ion batteries. *Electrochim Acta*. 2016;217:283-291.
 - [14] Hansen S, Quiroga-González E, Carstensen J, et al. Size-dependent physicochemical and mechanical interactions in battery paste anodes of Si-microwires revealed by fast-fourier-transform impedance spectroscopy. *J Power Sources*. 2017;349:1-10.
 - [15] Quiroga-Gonzalez E, Carstensen J, Föll H. Structural and electrochemical investigation during the first charging cycles of silicon microwire array anodes for high capacity Lithium ion batteries. *Materials*. 2013;6:626.
 - [16] Zhong L, Beaudette C, Guo J, et al. Tin nanoparticles as an effective conductive additive in silicon nodes. *Sci Rep*. 2016;6:30952.
 - [17] Choi HJ, Baek S, Jang HS, et al. Optimization of metal-assisted chemical etching process in fabrication of p-type silicon wire arrays. *Curr Appl Phys*. 2011;11: S25-S29.
 - [18] Li S, Ma W, Zhou Y, et al. Fabrication of porous silicon nanowires by MACE method in HF/H₂O₂/AgNO₃ system at room temperature. *Nanoscale Res Lett*. 2014;9:196-203.
 - [19] Noehren S, Quiroga-González E, Carstensen J, et al. Electrochemical fabrication and characterization of silicon microwire anodes for Li ion batteries. *J Electrochem Soc*. 2016;163:A373-A379.
 - [20] Boukamp BA, Lesh GC, Huggins RA. All-solid lithium electrodes with mixed-conductor matrix. *J Electrochem Soc*. 1981;128:725-729.
 - [21] Peng K, Fang H, Hu J, et al. Metal-particle-induced, highly localized site-specific etching of Si and formation of single-crystalline Si nanowires in aqueous fluoride solution. *Chem Eur J*. 2006;12:7942-7947.
 - [22] Tsujino K, Matsumura M. Morphology of nanoholes formed in silicon by wet etching in solutions containing HF and H₂O₂ at different concentrations using silver nanoparticles as catalysts. *Electrochim Acta*. 2007;53:28-34.
 - [23] Compton RG, Banks CE. Understanding voltammetry. London (UK): Imperial College Press; 2009.
 - [24] Obrovac M, Krause L. Reversible cycling of crystalline silicon powder. *J Electrochem Soc*. 2007;154:A103.
 - [25] Ge M, Rong J, Fang X, et al. Scalable preparation of porous silicon nanoparticles and their application for lithium-ion battery anodes. *Nano Res*. 2013;6:174-181.
 - [26] Alcántara R, Lavela P, Pérez-Vicente C, et al. Anode materials for lithium-ion batteries. In: Liu YX, Zhang J, editors. *Lithium-ion batteries advanced materials and technology*. New York (NY): CRC Press; 2012. p. 97-146.
 - [27] Chan CK, Ruffo R, Hong SS, et al. Structural and electrochemical study of the reaction of lithium with silicon nanowires. *J Power Sources*. 2009;189:34-39.